JOURNAL OF RAMAN SPECTROSCOPY, VOL. 27, 549–554 (1996)

Structure Characterization of WO_3/ZrO_2 Catalysts by Raman Spectroscopy

Biying Zhao,* Xianping Xu, Jinming Gao, Qiang Fu and Youqi Tang
Institute of Physical Chemistry, Peking University, Beijing 100871, China

WO_3/ZrO_2 catalysts prepared by different methods are distinct in their catalytic behaviour. In this work, WO_3/ZrO_2 catalysts prepared by impregnating $Zr(OH)_4$ and crystallized ZrO_2 and then calcining at selected temperatures were characterized by means of qualitative and quantitative Raman spectroscopy. The results showed that ZrO_2 in WO_3/ZrO_2 obtained from crystallized ZrO_2 (referred to as WZ) is monoclinic, whereas ZrO_2 in WO_3/ZrO_2 obtained from $Zr(OH)_4$ (referred to as WZH) is in a metastable tetragonal phase as long as the WO_3 content is high enough. In both WZ and WZH, WO_3 is dispersed on ZrO_2 as a monolayer, and the dispersion capacity per 100 m^2 of ZrO_2 is in good agreement with that estimated from the close-packed monolayer model. However, since the specific surface areas of WZH samples are larger than those of WZ samples, the dispersion capacity per gram of ZrO_2 of WZH is larger than that of WZ. A chemical reaction may occur between WO_3 and the surface of $Zr(OH)_4$ (or tetragonal ZrO_2) at high temperature, and then some superacid sites are created on the surface of the WZH sample.

INTRODUCTION

Any acid can be termed a superacid if its acidity is stronger than that of 100% H_2SO_4, i.e. $H_0 \leqslant -12.0$.[1,2] The catalytic activity of superacids is surprisingly high.[2] Solid superacids have some additional advantages as catalysts, e.g. no corrosion of the reactor and freedom from environmental problems in disposing of the used catalyst.[3] It is known that some sulphate-supported metal oxides are superacids.[3] In 1988, Arata and Hino[3–5] reported that solid superacid could also be synthesized by supporting WO_3 or MoO_3 on ZrO_2 under special preparation conditions. Since its active component is not easy to run off and it can remain stable at high temperatures and in a solid–liquid system, it may have better application prospects than those of the sulphate-promoted Fe_2O_3, TiO_2 and ZrO_2 superacids.

The main facts about the WO_3/ZrO_2 superacid system that have been reported so far are as follows:[4,5]

1. Superacid can be obtained only by impregnating amorphous $Zr(OH)_4$ instead of crystalline ZrO_2 with ammonium metatungstate solution.
2. It has been shown by x-ray diffraction that metastable tetragonal ZrO_2 is the major form in WO_3/ZrO_2 when $Zr(OH)_4$ is first impregnated with ammonium metatungstate solution and then calcined, whereas ZrO_2 obtained by calcining pure $Zr(OH)_4$ at the same temperature is monoclinic.
3. The sample calcined at 800 °C with a W content of 15 wt% has the greatest activity.

Many questions, particularly regarding the existing states of WO_3 in WO_3/ZrO_2, are still open. Our group reported[6,7] that the spontaneous monolayer dispersion of many oxides and salts on supports is a widespread phenomenon. When an oxide–support mixture is heated at a high enough temperature, it can usually be observed that the oxide has been dispersed on the surface of the support. The maximum monolayer dispersion capacity can be estimated by using the simple close-packed monolayer model.[6,7] However, is WO_3 dispersed on ZrO_2 as a monolayer in WO_3/ZrO_2 superacid? What is its dispersion capacity? How do the preparation conditions affect its structure? All of these problems are worth studying. In this work, the effects of the preparation method, the content of WO_3 and the calcination temperature on the structure of WO_3/ZrO_2 were studied by means of Raman spectroscopy. Their phase composition, including the surface dispersion phase, was studied by qualitative and quantitative Raman spectroscopy. The results obtained help in understanding much better the structure of this system.

EXPERIMENTAL

Sample preparation

Four groups of the samples were prepared from high-purity $ZrOCl_2 \cdot 8H_2O$ and $(NH_4)_6H_2W_{12}O_{40}$ according to the following procedures. The WO_3 contents in each group were 0.05, 0.10, 0.15, 0.20, 0.25, 0.30, 0.35, 0.40, 0.50 and 0.65 g per gram of ZrO_2.

$Zr(OH)_4$ precipitate was obtained by adding 3.3 M ammonia solution to 0.6 M $ZrOCl_2$ solution to give pH 9–10, then the resultant white precipitate was filtered and washed repeatedly with distilled water until the filtrate gave a negative test for Cl^- ions. The precipitate was heated at 120 °C for 24 h and then divided into two parts. One part was calcined at 500 °C for 12 h and then impregnated with solutions with predetermined amounts of ammonium metatungstate and calcined at

* Author to whom correspondence should be addressed.

CCC 0377–0486/96/070549–06

Received 19 October 1995
Accepted 10 March 1996

Table 1. Specific surface areas of the samples

WoO_3 content/g per gram of ZrO_2	Specific surface area/m^2 g^{-1} ZrO_2			
	WZ8	WZH8	WZ5	WZH5
0.05	54	55	69	78
0.15	52	75	65	172
0.25	47	66	63	205
0.30	45	60	61	220
0.35	41	58	59	239
0.40	—	41	—	251

500 or 800 °C for 12 h. The samples obtained were designated as WZ5 and WZ8, respectively.

The other part of $Zr(OH)_4$ heated only at 120 °C was impregnated with solutions of $(NH_4)_6H_2W_{12}O_{40}$, then dried and calcined at 500 or 800 °C for 12 h. The samples obtained were designated as WZH5 and WZH8, respectively.

The BET surface areas of the samples were determined by nitrogen adsorption at −196 °C using an ST-03 surface area–pore volume analyzer. The specific surface area of ZrO_2 calcined at 550 °C is 70 m^2 g^{-1}. The BET surface areas of the other samples are listed in Table 1.

The surface acidity of the sample was determined by using the Hammett indicator method. The samples were heated under a pressure of 10^{-2} Pa and at 450 °C for 1 h. After cooling, the samples were exposed to an indicator vapour. If some superacid sites exist with H_0 less than or equal to the pK_a of an indicator, the colour of the surface of the sample will change. The results showed that there were some superacid sites with $H_0 \leqslant -13.75$ on the surface of WZH8 (the indicator used was 2,4-dinitrotoluene with $pK_a = -13.75$). No superacid sites were found on the surfaces of WZH5, WZ5 and WZ8.

Raman spectroscopic analysis

Raman spectra were acquired on a Ramanor U-1000 double monochrometor with 1800 grooves mm^{-1} holographic gratings. A Spectra-Physics Stabilite-2016 argon ion laser was used to supply 514.5 nm exciting radiation. A power of *ca.* 100 mW was employed. The slit width was 1 cm^{-1}. The wavenumber accuracy of the recorded spectra was ±2 cm^{-1}. The powdered samples were pressed into wafers and rotated at high speed in order to reduce the damage of the heat effect on the sample.

In quantitative Raman determinations, KNO_3 was chosen as an internal standard.[8]

RESULTS AND DISCUSSION

Qualitative results

The Raman spectrum of pure ZrO_2 calcined at 800 °C is shown in Fig. 1(a). Comparison with a published spectrum[9] indicates that monoclinic ZrO_2 is dominant. Its characteristic peaks are at 220, 332, 380 474, 620 and 640 cm^{-1}. Figure 1(b), (c) and (d) show the Raman spectra of WZ8 samples with different WO_3 contents, from which we can see that monoclinic ZrO_2 is pre-

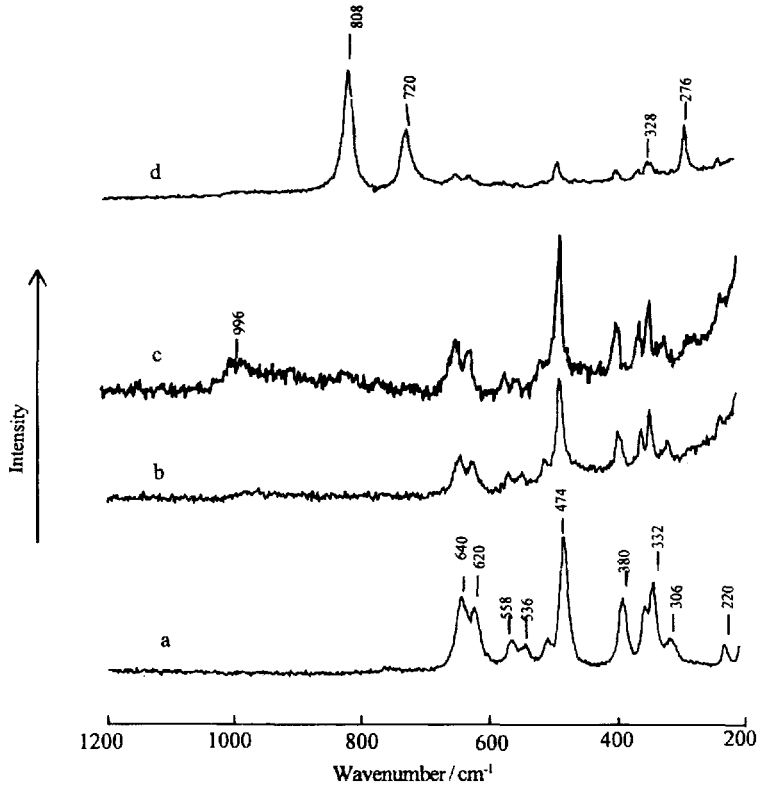

Figure 1. Raman spectra of WZ8 samples with different WO_3 contents. (a) ZrO_2; (b) 0.05 g WO_3; (c) 0.10 g WO_3; (d) 0.15 g WO_3 per gram of ZrO_2.

dominantly present, there is a broad band at 996 cm^{-1} and the greater the content of WO_3, the larger is the area of this band. Referring to published spectra of WO_3/TiO_2 and WO_3/Al_2O_3,[10–12] we can recognize that it is the characteristic band of a monolayer dispersion of WO_3, and is due to the symmetrical stretching mode of W=O. Further, the characteristic peaks of crystalline WO_3 [11,12] (808, 720, 328 and 276 cm^{-1}) appear when the content of WO_3 is beyond a certain level.

These results are proof that WO_3 can be dispersed on ZrO_2 in a monolayer dispersion state, and crystalline WO_3 appears only when the content of WO_3 is beyond the monolayer capacity of WO_3 on ZrO_2.

A similar phenomenon occurs in the WZ5 series calcined at 500 °C (see Fig. 2). What is different is that besides the monolayer dispersion phase, a small amount of crystalline WO_3 can be detected even in the samples with low WO_3 contents (i.e. 0.05 and 0.10 g WO_3 per gram of ZrO_2). The reason might be that if part of the $(NH_4)_6H_2W_{12}O_{40}$ decomposes before being dispersed completely and forms crystalline WO_3, the resultant crystalline WO_3 would disperse further during calcination at 800 °C. However, as the samples are calcined at 500 °C, the dispersion of the crystalline WO_3 is difficult owing to its high melting point and therefore it remains crystalline in the samples. Moreover, it should be noted that the band of monolayer WO_3 shifts to *ca.* 962 cm^{-1}. This phenomenon demonstrates that the wavenumber of the monolayer band depends on the calcination temperature, which is in agreement with the literature.[10,12]

Figure 3 shows the Raman spectra of WZH8 samples that are similar to those of WZ8 in some ways: there is only a broad band at 996 cm^{-1} which represents the monolayer dispersion phase when the content of WO_3 is below its monolayer capacity. The characteristic peaks of crystalline WO_3 appear only when the content of WO_3 is higher than a certain level. However, there are some differences between WZH8 and WZ8:

(a) A considerable portion of ZrO_2 exists in a metastable tetragonal phase, and its characteristic peaks at about 268, 325, 478 and 648 cm^{-1} (Ref. 9) are rather broad. The overall spectrum is different from that of monoclinic ZrO_2, and the peaks at 268 and 325 cm^{-1} and those of monoclinic ZrO_2 do not overlap, and so they can be used as standards to determine the existence of metastable tetragonal ZrO_2 in the system and to estimate its content. From Fig. 3, it can be seen that a considerable amount of monoclinic ZrO_2 exists in the sample with a WO_3 content of 0.10 per gram of ZrO_2. However, the tetragonal ZrO_2 is predominantly present when the content of WO_3 is 0.15 g per gram of ZrO_2. There are similar characteristics in WZH5.

It has been reported[13] that ZrO_2 can exist in three phases: monoclinic, tetragonal and cubic. The monoclinic ZrO_2 is stable below 1170 °C, the tetragonal phase is observed at 1170–2370 °C and the cubic phase is stable from 2370 °C up to its melting point. However, the tetragonal phase ZrO_2(t) is stabilized by a crystallite size effect,[14] i.e. it can be stable from room temperature to 1170 °C provided that its crystallites are below a certain critical size. In this case, it is referred as metastable tetragonal ZrO_2.

Zirconia, the catalyst support, involves mainly two phases: ZrO_2(m) and metastable tetragonal ZrO_2.[9] With a small size, the metastable tetragonal ZrO_2 has a larger specific surface area, and its Raman peaks are broader. This is the case for WZH samples.

(b) In addition to the characteristic peaks of crystalline WO_3, a small peak at 580 cm^{-1} can be observed when the WO_3 content of the sample is more than 0.20 g per gram of ZrO_2. This peak is not observed in the spectra of samples of WZ5, WZ8 and WZH5. This peak appears only in the sample prepared by using $Zr(OH)_4$

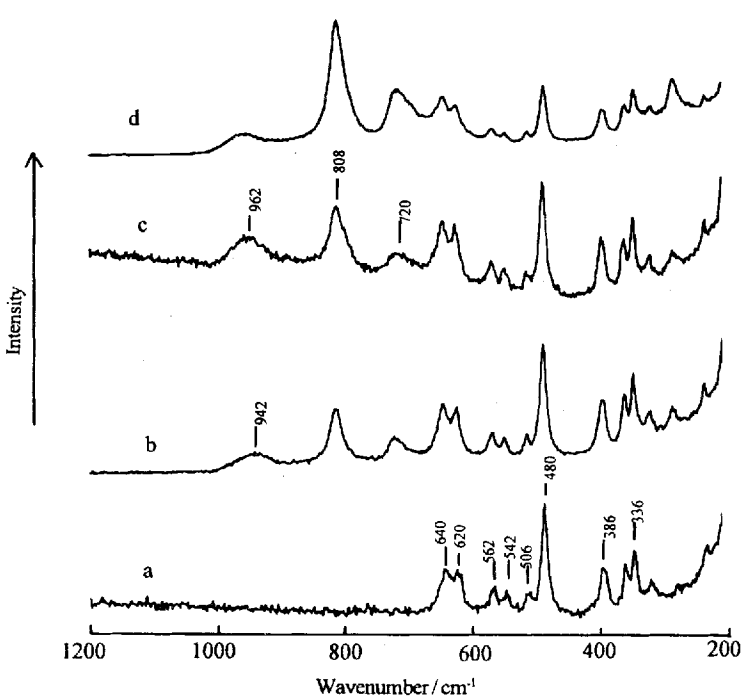

Figure 2. Raman spectra of WZ5 samples with different WO_3 contents. (a) ZrO_2; (b) 0.05 g WO_3; (c) 0.10 g WO_3; (d) 0.15 g WO_3 per gram of ZrO_2.

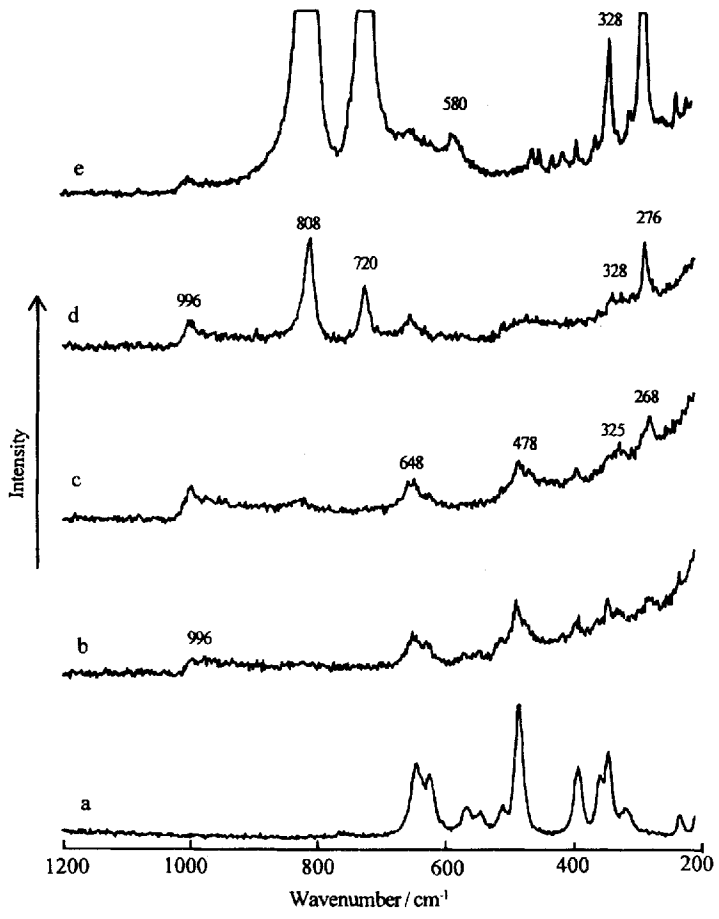

Figure 3. Raman spectra of WZH8 samples with different WO_3 contents. (a) ZrO_2; (b) 0.10 g WO_3; (c) 0.15 g WO_3; (d) 0.20 g WO_3; (e) 0.30 g WO_3 per gram of ZrO_2.

as support and then calcining at 800 °C. We think that a new W—O—Zr species might be formed between WO_3 and ZrO_2 under the preparation conditions used, and it might be responsible for the superacidity of WZH8. This phenomenon is more obvious in the MoO_3/ZrO_2 system.[15] This might be why there are no superacid sites in WZH5 although ZrO_2 in them is tetragonal, and a larger amount of dispersed WO_3 can be accommodated owing to their high specific surface areas.

Quantitative measurement

KNO_3 was used as an internal standard[8,16] and mixed with the sample in an appropriate ratio. The peak areas of monolayer WO_3 at 996 cm^{-1}, crystalline WO_3 at 808 cm^{-1} and KNO_3 at 1050 cm^{-1} were measured, and then normalized as the peak-area ratios of the first two peaks to the last peak as there are equal amounts of KNO_3 and ZrO_2 in the sample. The ratios are regarded as the relative contents of monolayer dispersion and crystalline WO_3 phase. The spectra were accumulated several times. Figure 4 shows an example.

Figure 5 gives the quantitative Raman results for WZ8 and WZH8 samples. It can be seen that when the content of WO_3 in WZ8 is low, WO_3 exists in the form of a monolayer phase, the content of which increases with increase in WO_3 content. After the content of WO_3 has reached a certain value, the content of the monolayer phase does not change and crystalline WO_3 appears, and its content increases gradually with increase in total WO_3 content. The plots showing the relationship between the relative content of monolayer WO_3, the relative content of crystalline WO_3 *vs.* total WO_3 content, exhibit a change of slope which occurs at the same total WO_3 content. At this point, the maximum monolayer capacity is 0.11 g WO_3 per gram of ZrO_2, i.e. 0.20 g WO_3 per 100 m^2 of ZrO_2 (the surface area of the sample is 52 $m^2\ g^{-1}$), which is consistent with the theoretical close-packed monolayer dispersion capacity, 0.19 g per 100 m^2 of ZrO_2.[6,7] This result indicates that WO_3 can form a nearly perfect monolayer on the surface of ZrO_2.

The quantitative result for WZH8 [see Fig. 5(b)] is similar to that for WZ8. The change of slope corresponds to a WO_3 content of 0.17 g per gram of ZrO_2, which seems higher than that of WZ8. However, the surface area of the sample is about 75 $m^2\ g^{-1}$ ZrO_2, and therefore the monolayer capacity is about 0.23 g WO_3 per 100 m^2 of ZrO_2, only slightly higher than its theoretical capacity. We have noted that the change of point of the quantitative curve of the monolayer phase is not so definite for WZH8, and the content of the monolayer phase decreases slowly with increasing WO_3 content when the total content of WO_3 is above the threshold. The small band at 580 cm^{-1} in the Raman spectra of this series of samples may be due to the formation of a new species that is produced by the reaction between $Zr(OH)_4$ (or tetragonal ZrO_2) and the active component at 800 °C.

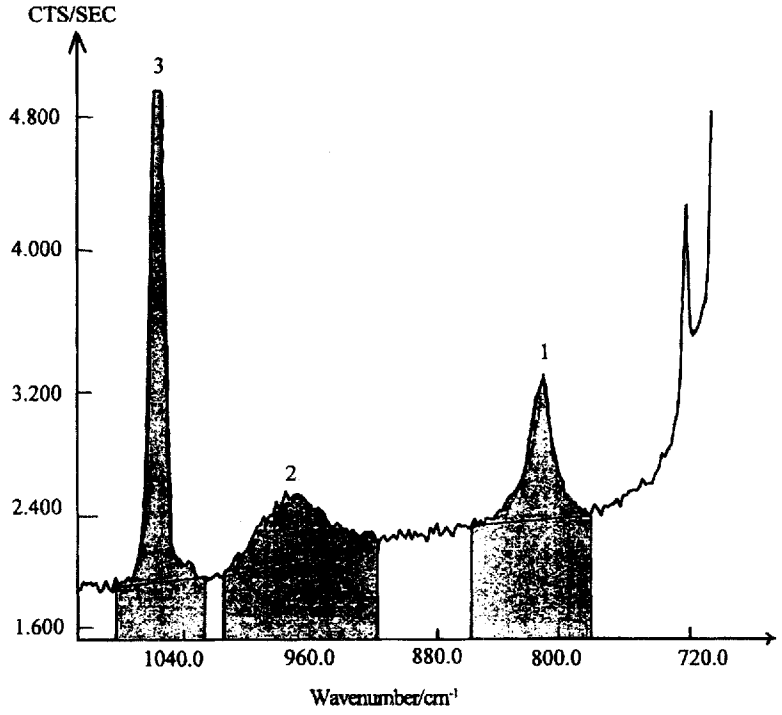

Figure 4. Representative example of quantitative Raman results for WO_3/ZrO_2. (1) The band of crystalline WO_3 at 808 cm^{-1}; (2) the band of monolayer WO_3 at 996 cm^{-1}; (3) the band of KNO_3 at 1050 cm^{-1}.

The quantitative Raman curves for the WZ5 and WZH5 series of samples are similar to those of the WZ8 series, the only difference being that the characteristic peak of crystalline WO_3 appears when the content of WO_3 is lower than the threshold derived from the quantitative curve. As stated above, this is because the dispersion equilibrium has not really been established in the system calcined at 500 °C.

CONCLUSIONS

ZrO_2 in WO_3/ZrO_2 obtained by impregnating crystallized ZrO_2 is monoclinic, but in WO_3/ZrO_2 obtained by impregnating $Zr(OH)_4$ it is metastable tetragonal provided that WO_3 content is high enough.

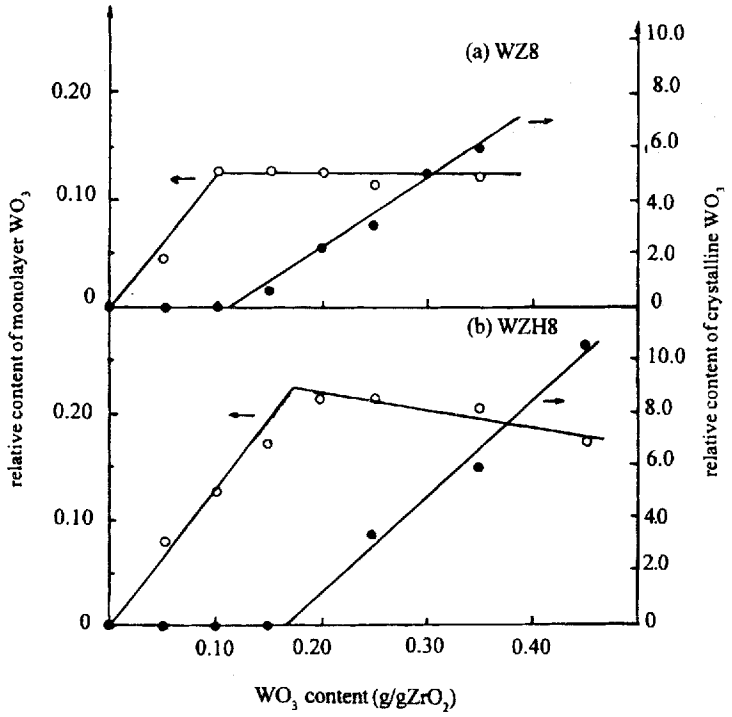

Figure 5. Contents of monolayer WO_3 and crystalline WO_3 *vs.* total contents of WO_3 in WO_3/ZrO_2.

WO_3 in WO_3/ZrO_2 exists on the surface of ZrO_2 as a monolayer phase no matter whether ZrO_2 or $Zr(OH)_4$ is used in the impregnation process, and its dispersion threshold is in agreement with the theoretical close-packed monolayer dispersion capacity.

Some kind of chemical binding is formed between $Zr(OH)_4$ (or tetragonal ZrO_2) and WO_3 at high temperature. This might be responsible for the superacidity of the sample prepared by impregnating $Zr(OH)_4$ and then calcining it at 800 °C.

Acknowledgement

Funding for this research was provided by the National Natural Science Foundation, China.

REFERENCES

1. R. J. Gllespie and T. E. Peel, *Adv. Phys. Org. Chem.* **9**, 1 (1972).
2. G. A. Olah, G. K. S. Prakash and J. Sommer, *Science* **206**, 13 (1979).
3. K. Arata, *Adv. Catal.* **37**, 165 (1990).
4. M. Hino and K. Arata, *J. Chem. Soc., Chem. Commun.* 1259 (1988).
5. K. Arata and M. Hino, in *Proceedings of the IXth International Congress on Catalysis, Calgary*, edited by M. J. Phillips and M. Ternan, Vol. IV, p. 1727. Chemical Institute of Canada, Calgary (1988).
6. Y. Xie, L. L. Gui, Y. J. Liu, B. Y. Zhao, N. F. Yang, Y. F. Zhang, Q. L. Guo, L. Y. Duao and Y. Q. Tang, in *Proceedings of the 8th International Congress on Catalysis*, Vol. 5, p. 147, Verlag Chemie, Berlin (1984).
7. Y. C. Xie and Y. Q. Tang, *Adv. Catal.* **37**, 1 (1990).
8. J. P. Baltrus, L. E. Makovsky, J. M. Stencel and D. M. Hercules, *Anal. Chem.* **57**, 2500 (1985).
9. P. D. L. Mercera, J. G. van Ommen, E. B. M. Doesburg, A. J. Burggraaf and J. R. H. Ross, *Appl. Catal.* **57**, 127 (1990).
10. S. S. Chan, I. E. Wachs, L. L. Murrell and N. C. Dispenziere, Jr, *J. Catal.* **92**, 1 (1985).
11. M. J. Stencel, *Raman Spectroscopy for Catalysis*. Van Nostrand Reinhold, New York (1989).
12. L. Dixit, D. L. Gerrad and H. J. Bowley, *Appl. Spectrosc. Rev.* **22**, 189 (1986).
13. E. C. Subbarao, H. S. Maiti, K. K. Srivastava, *Phys. Status Solidi A* **21**, 9 (1974).
14. R. C. Garvie and M. F. Goss, *J. Mater. Sci.* **21**, 1253 (1986).
15. B. Y. Zhao and H. R. Ma, *J. Catal. (China)* **16**, 171 (1995).
16. B. Y. Zhao, Q. Xu, Y. C. Xie and X. C. Yang, *Chem. J. Chin. Univ.* **11**, 54 (1990).